

Chiral and non-chiral swift mode conversion near an exception point with dynamic adiabaticity engineering

Dong Wang^{1,2,3,4,6}, Wen-Xi Huang^{5,6}, Pei-Chao Cao^{1,2,3,4}, Yu-Gui Peng⁵, Xue-Feng Zhu^{5*}, Ying Li^{1,2,3,4*}

¹*Interdisciplinary Center for Quantum Information, State Key Laboratory of Extreme Photonics and Instrumentation, ZJU-Hangzhou Global Scientific and Technological Innovation Center, Zhejiang University, Hangzhou 310027, China.*

²*International Joint Innovation Center, The Electromagnetics Academy at Zhejiang University, Zhejiang University, Haining 314400, China*

³*Key Lab. of Advanced Micro/Nano Electronic Devices & Smart Systems of Zhejiang, Jinhua Institute of Zhejiang University, Zhejiang University, Jinhua 321099, China*

⁴*Shaoxing Institute of Zhejiang University, Zhejiang University, Shaoxing 312000, China*

⁵*School of Physics and Innovation Institute, Huazhong University of Science and Technology, Wuhan 430074, China.*

⁶*These authors contributed equally: Dong Wang, Wen-Xi Huang*

* e-mail: xfzhu@hust.edu.cn; eleying@zju.edu.cn

The eigenvalue of a non-Hermitian Hamiltonian often forms a self-intersecting Riemann surface, leading to a unique mode conversion phenomenon when the Hamiltonian evolves along certain loop paths around an exceptional point (EP). However, two fundamental problems exist with the conventional scheme of EP encircling: the speed of mode conversion is restricted by the adiabatic requirement, and the chirality cannot be freely controlled. We introduce a method for dynamically engineering adiabaticity in the evolution of non-Hermitian Hamiltonians that allows for both chiral and non-chiral mode conversion on the same path. Our method is based on quantifying and controlling the instantaneous adiabaticity, allowing for non-uniform evolution throughout the entire path. By optimizing the evolution based on the distributed nature of adiabaticity, we achieve the same quality as conventional quasi-adiabatic evolution in only one-third of the time. Our approach provides a comprehensive and universal solution to address the speed and chirality challenges associated with EP encircling. It also facilitates the dynamic manipulation and regulation of non-adiabatic processes, thereby accelerating the operation and allowing for a selection among various mode conversion patterns.

The Hamiltonian of a system determines its state and time evolution. In open systems whose effective Hamiltonian are non-Hermitian, an intriguing form of degeneracy, the exceptional point (EP) may exist, where both the eigenvalues and eigenstates coalesce[1]. To date, many unusual properties about the EP have been discovered, which can be implemented for single-mode lasing [2][3], loss-induced transmission enhancement [4], unidirectional invisibility [5][6], enhanced sensing [7]-[10], etc.

The eigenvalue of a non-Hermitian Hamiltonian is often complex and forms a self-intersecting Riemann surface. As a result of this unique geometry, when the Hamiltonian evolves along certain loop path around an EP, the initial eigenstate cannot be recovered after completing the loop [11]. A mode conversion can thus be achieved by adiabatically encircling an EP. For Hermitian Hamiltonians, the adiabatic condition can be reached at a sufficiently slow evolution speed. However, for non-Hermitian Hamiltonians, a slow evolution can only guarantee adiabatic evolution on the uppermost imaginary Riemann sheet [12], where the eigenvalue has the largest imaginary part and the eigenstate has the smallest decay rate. Therefore, the mode switching only works in one direction (*e.g.* counterclockwise, CCW). If the Hamiltonian evolves in the opposite direction (*e.g.* clockwise, CW), it goes to a lower imaginary Riemann sheet but cannot be maintained there. A nonadiabatic jump to the uppermost sheet will happen and the initial state is recovered after completing the loop. This asymmetric mode conversion phenomenon uncovers the chirality of EP encircling, and has aroused great research interests with a variety of potential applications like optical communications [13], quantum control [14], and optical isolators [15].

Despite the rich results, two fundamental problems still exist with the scheme of EP encircling. First, the speed of mode conversion is restricted by the adiabatic requirement. The slow evolution may not only influence the efficiency of operation, but also lead to strong decay of the mode. To overcome the problem, recent works proposed a discontinuous encircling protocol via Hamiltonian hopping [16] and a selected loop along the parameter space boundary [17] to accelerate the evolution procedure. However, the methods require a Hamiltonian with extreme parameters and low-loss eigenstates along the path, which hinder their application to the general situations.

Another problem with EP encircling is that the chirality cannot be freely controlled. To elaborate the issue, let us consider the typical case of a two-level Hamiltonian, and name the two

eigenstates at the starting point as modes A and B. For simplicity, the starting point is chosen at the branch cut of the imaginary Riemann surface. Assuming that mode A is the initial state, there are three possibilities after CCW and CW evolutions. (1) Chiral mode conversion: mode A \rightarrow B (CCW), mode A \rightarrow A (CW). (2) Non-chiral mode recovery: mode A \rightarrow A (CCW and CW). (3) Non-chiral mode conversion: mode A \rightarrow B (CW and CCW). The conventional scheme can only realize chiral mode conversion (1). Recently, it has been shown that by evolving along a loop path that does not encircle an EP, both chiral mode conversion (1) and non-chiral mode recovery (2) can be realized [18]. However, the outcome depends on the details of the loop path. In addition, the non-chiral mode conversion (3) has not been observed yet.

In short, the speed and chirality problems with EP encircling have only been considered by a few works, whose partial solutions rely on specific models (evolution paths or Hamiltonians). Therefore, a general and complete recipe is in great demand. We believe that adiabaticity is the key to fully resolve both problems, but it has not gain sufficient attention yet. In conventional schemes, the state is maintained close to the Riemann surface throughout the encircling operation, except for the unavoidable jumps. This approach preserves a global quasi-adiabaticity, but has overlooked the degree of adiabaticity at each instant. To date, a systematic method to quantify and control the instantaneous adiabaticity is still missing, so is the potentially abundant space for efficiency optimization. Another overlooked aspect is the absence of adiabaticity. Previous schemes either avoid non-adiabatic processes (in the mode conversion operation) or have to wait for the non-adiabatic jump between Riemann sheets (in the mode recovery operation). Rare efforts have been made to actively introduce and control such processes at will. As a result, an important tool is lacked to further speed up the operation and choose freely among different mode conversion patterns.

Here, we present the method of dynamic adiabaticity engineering for the evolution of non-Hermitian Hamiltonians. Compared to conventional quasi-adiabatic evolution, the optimized evolution with our method achieves the same quality in only one-third of the time. Furthermore, our method allows for both chiral and non-chiral mode conversion on the same path. By considering the distributed nature of adiabaticity along a given parameter path, quantifying adiabaticity enables the realization of non-uniform evolution throughout the entire path, whereby the velocity at each local point along the evolution path is optimized through adiabaticity. This quantification also obviates the need for a strict dichotomy between adiabatic and non-adiabatic processes, as they can be incorporated within the same framework based on their respective adiabaticity. Notably, our proposed methodology allows the system state to deviate from the Riemann surface, in contrast to conventional options of either strictly adhering to it or performing jumps between two surfaces. Our work not only enriches our understanding of the adiabaticity property in non-Hermitian systems but also offers valuable insights for advancing the application of mode converters. The dynamic adiabaticity engineering method presents a promising avenue for achieving efficient and high-quality evolution of non-Hermitian systems.

Non-uniform dynamic evolution

In the study of general chiral phenomena, to complete the switching of the initial mode, the state needs to evolve cling to the upper Riemann surface of the imaginary part. This process is usually achieved by evolving at a sufficiently slow speed of parameter change. To quantify this evolving speed, we define a function $C(x, y)$ which satisfies the planar geometric relationship to represent the position of the system on a certain parameter path: $dC^2(x, y) = (dx^2 + dy^2)/\rho$, $\int_C dC = 1$, where ρ is the normalization factor. Therefore, the speed of parameter change is defined as: $v =$

dC/dt . In general research, the system generally moves at a uniform speed v_0 on the parameter path, as shown in Fig. 1(a). However, the uniform evolution is not the optimal solution to achieve mode switching because the adiabaticity is not uniform during the evolution process. With this consideration, we could design the nonuniform evolution speed $v(t)$, which depends on the adiabatic requirement along the path: the high (low) adiabaticity demands the low (high) speed. Undoubtedly, this treatment can accelerate the switching process (Fig. 1b). It seems that this adiabaticity-dependent evolution scheme is the fastest method to realize mode conversion, if the adiabaticity must be preserved during the whole evolution path. Nevertheless, many realistic problems implicate huge demand to rapidly evolve to the target steady state, such as stochastic heat engines [19] and probability distribution of genotypes in a population [20]. When we care more about the effect of mode conversion, the process can be faster as long as we abandon the adiabaticity of a certain evolution path. This opinion is illustrated vividly in Fig. 1c. Physically, these three different evolution forms can be signified in the projection plane of Riemann surface. In this study, we consider a non-Hermitian system with EP:

$$\hat{H} = \begin{pmatrix} x + iy & 1 \\ 1 & -x - iy \end{pmatrix}. \quad (1)$$

Here $x, y \in \mathbb{R}$. Most of the two-level system can be transformed into this form. The Riemann surface of imaginary eigenvalues is shown in Fig. 1d. The conventional study of dynamically encircling EP corresponds the process in which v is constant in the projection plane (upper in Fig. 1e), while the non-uniform and “jump” processes are shown in Fig. 1e as well (middle and lower respectively).

Adiabaticity engineering

To study and compare the three dynamic evolution paradigms above, it is necessary to quantify adiabaticity. At first, system's state at each time is obtained approximately by difference iteration after discretization:

$$|\Psi_j\rangle = \sum_n c_{n,j} |\psi_{n,j}\rangle, \quad (2)$$

$$|\Psi_{j+1}\rangle = \sum_n \langle \theta_{n,j+1} | \Psi_j \rangle e^{-i\omega_{n,j+1}\Delta t_j} |\psi_{n,j+1}\rangle. \quad (3)$$

Here, $\{\langle \theta_n | \}$ and $\{|\psi_n\rangle\}$ are the normalized biorthogonal basis of the non-Hermitian Hamiltonian, subscript n is sorted from the largest to the smallest according to the imaginary part of the eigenvalue, subscript j represents the j th parameter point, Δt_j is the evolving time in the j th parameter point, $c_{n,j}$ is the coefficient of eigenstate $\psi_{n,j}$, $\omega_{n,j+1}$ is the corresponding eigenvalue of eigenstate $|\psi_{n,j+1}\rangle$, $\langle \theta_{n,j+1} | \Psi_j \rangle e^{-i\omega_{n,j+1}\Delta t_j}$ actually stands for $c_{n,j+1}$. We use the weighted eigenvalue $\bar{\omega}_j$ of system's state to characterize system's state in Riemann surface:

$$\bar{\omega}_j = \sum_n \frac{|c_{n,j}|^2}{\sum_m |c_{m,j}|^2} \omega_{n,j}. \quad (4)$$

Then we could define the proportion $P_{n,j}$ of the instantaneous eigenstate $|\psi_{n,j}\rangle$: $P_{n,j} = |c_{n,j}|^2 / \sum_m |c_{m,j}|^2$. In general, the adiabatic evolution requires the system to be mainly in the least decaying state. Here, it means the proportion $P_{1,j}$ of a set of instantaneous eigenstates with the largest imaginary parts should not be lower than a certain value during the entire evolution time. We name $P_{1,j}$ as the dominant state proportion. The lower limit of the proportion is set to P_0 ($P_{1,j} \geq P_0$). The larger P_0 indicates the high adiabaticity. In our study, P_0 is set to 0.9.

With the preset above, we can calculate the residence time Δt_j in each parameter point on the evolution path. When the current state $|\psi_j\rangle$ is given, the dominant state proportion at the next parameter point is:

$$P_{1,j+1} = \frac{|\langle \theta_{1,j+1} | \psi_j \rangle e^{-i\omega_{1,j+1} \Delta t_j}|^2}{\sum_n |\langle \theta_{n,j+1} | \psi_j \rangle e^{-i\omega_{n,j+1} \Delta t_j}|^2}. \quad (5)$$

Then we let $P_{1,j+1} = P_0$ (adiabatic evolution requirement), which turns to be a single variable equation with variable Δt_j . We could obtain Δt_j of each parameter point with this equation, therefore the evolution time set $\{\Delta t_j\}$ is figured out. Since this evolution is based on the dynamic modulation of the dominate proportion, which indeed can constrain the purity of end state, we call it the “stable conversion configuration” in this paper.

The mode conversion results of the stable conversion configuration (nonuniform evolution) are given in Fig. 2. The evolution time set $\{\Delta t_j\}$ and evolution picture are shown in Fig. 2a and 2b. The parameter path is subdivided into 100 equal intervals and there are 101 parameter points in total. In the beginning, the dominant state proportion is larger than P_0 , so this evolutionary path can actually be skipped until it falls to P_0 . We have calculated two different input modes and two different evolution directions. The four cases are shown in Fig. 2c-2f in which the $\zeta_{A,B}$ is the coefficient of mode A or B: $\zeta_{A,B;j} = |\langle \theta_{A,B} | \psi_j \rangle|^2 / \sum_{A,B} |\langle \theta_{A,B} | \psi_j \rangle|^2$. The chiral mode switching effects are realized for both input modes. Notably, this bimodal chiral evolution has not been achieved in previous research. As a comparison, we also give the case of uniform evolution. For mode A, we have not only realized the faster mode conversion, but also maintained the high purity of the end state (Fig. 2c). However, for mode B, the transfer effect is not ideal (Fig. 2e). The reason is that the parameter path skipped at the beginning of the counterclockwise (CCW) evolution

becomes the last path of clockwise (CW) evolution and the evolution time set $\{\Delta t_j\}$ is based on CCW evolution. To optimize the effect of CW dynamic evolution, additional constraints need to be considered.

Demand-driven strategy for dynamical evolution

In the dynamic evolution, focusing on the adiabaticity in the evolutionary process can always maintain the purity state, but in many cases, the high adiabatic confinement is unnecessary to be satisfied during the entire parametric path. For example, in the case of mode switch, as long as the purity of the end state after switching is high enough, some properties like adiabaticity during the procedure along the path does not really count (Fig. 1c). This cognition inspires us to propose a general scheme of dynamic evolution to achieve arbitrary mode conversion effect for arbitrary input, as well as keeping the high purity at the same time. Through the stable conversion configuration mentioned above, we can summarize two conditions the system exhibits during evolving: I. Jumping from a certain parameter point to another, which is instantaneous; II. Statically evolving in the parameter point for Δt_j . Generally, procedure I has abandoned the adiabaticity in some certain evolution path while procedure II is just the compensation. The appropriate combination of jumping points and statically evolving points with evolving time set $\{\Delta t_j\}$ determines the optimized results of dynamic evolution with typical demand. Therefore, all of the dynamic evolution problems can be reduced to a certain optimization problem in our framework, the differences among them are constraints we set in the optimization. In this paper, the constraints are summarized as: I. A certain enclosed parameter path; II. Evolutionary direction (CCW or CW); III. Input mode; IV. End state and its purity.

Model of the optimization. Firstly, we divide the path into J parts (in this study, $J=100$. The size of J will affect the iterative accuracy of evolution, and should not be too small). Four integer variables j_1, j_2, j_3, j_4 are defined to satisfy $1 \leq j_2 \leq j_3 \leq j_4 \leq J$. Then, path j_1 to j_2 and j_3 to j_4 are divided into N_1 aliquot (in this study, $N_1 = 5$) respectively, each aliquot path is assigned a decimal variable Δt to evolve. There are 4 integer variables and $2N_1$ decimal variables in total. This model design is based on our pre-calculation, which indicates that in the optimal results, most of the parameter paths are skipped. Hence the computational overhead will be reduced in this treatment. In more general cases, we can choose different partition according to different Hamiltonian.

Considering that this model involves integer variables and decimal variables, and in order to reduce the interference caused by the possible local optimal solution, we choose the joint algorithm of genetic algorithm [21] and SQP (Sequential Quadratic Programming) algorithm [22]. The genetic algorithm provides the initial values of all variables. The SQP algorithm optimizes the decimal variables within a given range, then returns the time consumption to the objective function of the genetic algorithm, and sets up multiple populations at the outermost layer and adds population migration. The algorithm flow is shown in Table 1.

Table 1: Genetic-SQP Algorithm

1. **Begin GA:** Randomly generate initial population (5 subpopulations) and open parallel pools
2. **Repeat:** {
3. Use fmincon function for parallel optimization to obtain the fitness value of individual.
4. RETURN fitness values to the GA.
5. Perform crossover automatically. }
6. **Until:** The fitness values before and after are the same.

7. Compare the optimal individual fitness of each subpopulation.
8. **If** {fitness is different}:
9. Population Migration: replace some of the worst individuals of the next subpopulations with some of the best individuals of the previous subpopulations to generate a new population.
10. Go to Step 2.
11. **Else:**
12. RETURN 1: integer parameters of the best individual.
13. Use fmincon function to optimize the decimal parameters of the best individual.
14. RETURN 2: decimal parameters.

Swift bimodal chiral evolution

To verify the superiority of our algorithm, we still perform the bimodal chiral evolution, whose results are illustrated in Fig. 3e-3f and the evolution processes of CCW and CW in the parameter plane are shown in Fig. 3a-3b. We find that systems skipped most areas of the evolutionary path and stayed in some specific parameter points. Indeed, this parametric jump is instantaneous and the system does not change in the representation of mode A/B. The mode-switch and mode-stay are the consequences of statically evolving at typical points, which can be considered as the results of adiabaticity compensation as well. The adiabaticity is modulated by these jump and stagnation and thus it will reduce the evolution time to a great extent. Compared with uniform evolution, we find that all of the four cases exhibit faster effects (mode switching or mode maintaining) and higher purity of end states, which confirm our assumption. It is worth noting that these “perfect” results are comprehensive because they are just originated from the constraints we set in our evolution framework. Moreover, we have designed the chiral index (CI) to characterize how good the chiral mode switching effect is. In our study, CI is the arithmetic average of $\zeta_{A,B}$ for end states

in CCW and CW: $CI = \frac{1}{2} \max\{(\zeta_{A;\text{end}}, \zeta_{B;\text{end}})|_{\text{CCW}}\} + \frac{1}{2} \max\{(\zeta_{A;\text{end}}, \zeta_{B;\text{end}})|_{\text{CW}}\}$. The chiral effects of uniform evolution, stable conversion configuration and Genetic-SQP Algorithm Optimization for different input modes are illustrated in Fig. 3g. We find that both stable conversion and Genetic-SQP methods present better chiral effects compared with uniform evolution. Besides, an advantage of Genetic-SQP method over stable conversion method is that it is independent of the input mode, which provides more potential for chiral converters to become practical.

Swift bimodal non-chiral evolution

The dynamic evolution framework we introduced above is named as “Stable and fast dynamic evolution configuration” and the chiral mode conversion effect has been demonstrated with swift transition, high purity and marvelous chiral index and at the same time. It should be pointed out that, our method is a demand-orientated framework to realize dynamic evolution near EP. In addition to the chiral evolution, we can also achieve any other dynamic evolution effects as long as the corresponding constraints are added in the optimization pool. To illustrate this, the non-chiral evolution effects are implemented, which are show in Fig. 4. Notably, we refer “chiral” as the distinguishing phenomena evolving in CCW and CW here so the non-chiral evolution indicates that the output modes are the same for a specific encircling path even if the evolution directions (CW or CCW) are different. For mode A, we have realized the mode conversion in both CCW and CW evolution (Fig. 4c-4d), which is called the bidirectional mode conversion. While for mode B, the non-chiral evolution is observed as well (Fig. 4e-4f), in which the mode B are stayed in both CCW and CW directions. This intriguing phenomenon are essentially different from the traditional

work about dynamically encircling EP because it breaks our perceptions that in the dynamic evolution around EP, only the chiral results will occur. In addition, the optimized evolutionary pictures (Fig. 4a-4b) still skipped most areas of the evolutionary path to realized faster mode conversion. This evolutionary behavior can be illustrated in the imaginary Riemann surfaces as well (Fig. 4g-4h, which is relevant to the bidirectional mode conversion in Fig. 4c-4d), from which we can find the balancing between freeing adiabaticity and keeping the state's purity along the path. Notably, even if the system has not evolved in some parameters, $\bar{\omega}$ will still change due to the change of the instantaneous eigenvectors, so on the skipped parameter path, $\text{Im}(\bar{\omega})$ is fluctuating. While on the parameter path the system stays, $\text{Im}(\bar{\omega})$ is increasing. In order to underscore the advantages of our approach in time-consuming, the evolution time required for achieving different final state switching proportions by three methods, namely, Uniform evolution, Stable conversion and Genetic-SQP algorithm optimization under different final state purity requirements, is shown in Fig. 4i. It can be seen that compared with the first two evolution methods, the time consumption of Genetic-SQP algorithm optimization method is greatly reduced, and with the change of final state purity constraint, the time consumption growth is not significant. The higher the final purity requirement is, the more significant the advantage of this method.

In conclusion, we have shown that in the dynamic evolution of non-Hermitian systems, the adiabaticity along the parameter loop is not necessarily to be conformed all the time if we pay more attention to the mode conversion results or the chiral effect. Based on this consideration, we have proposed a general evolutionary framework to realized arbitrary effects of mode conversion, mode maintaining, chiral and non-chiral evolution phenomena with any final state purity requirement, as long as the demand-orientated constraints are thrown into the optimization pool. In contrast to traditional encircling approaches, our analytical and computational configuration is

fast, model-independent and can be used to obtain arbitrary effect like chiral and non-chiral swift mode conversion, thereby enriches and deepens the understanding of non-Hermitian dynamic evolution and adiabatic theory in Riemann surfaces. Moreover, our work has promoted the application of chiral convertor in terms of computational resources, model fitness and results reconfiguration.

References

- [1] T.Kato, *Perturbation Theory for Linear Operators* (Springer, New York, 1966).
- [2] H. Hodaei, M.-A. Miri, M. Heinrich, D. N. Christodoulides, and M. Khajavikhan, Parity-Time–Symmetric Microring Lasers, *Science* 346, 975 (2014).
- [3] L. Feng, Z. J. Wong, R.-M. Ma, Y. Wang, and X. Zhang, Single-Mode Laser by Parity-Time Symmetry Breaking, *Science* 346, 972 (2014).
- [4] A. Guo, G. J. Salamo, D. Duchesne, R. Morandotti, M. Volatier-Ravat, V. Aimez, G. A. Siviloglou, and D. N. Christodoulides, Observation of P T -Symmetry Breaking in Complex Optical Potentials, *Phys. Rev. Lett.* 103, 093902 (2009).
- [5] L. Feng, Y.-L. Xu, W. S. Fegadolli, M.-H. Lu, J. E. B. Oliveira, V. R. Almeida, Y.-F. Chen, and A. Scherer, Experimental Demonstration of a Unidirectional Reflectionless Parity-Time Metamaterial at Optical Frequencies, *Nature Mater* 12, 108 (2013).
- [6] Z. Lin, H. Ramezani, T. Eichelkraut, T. Kottos, H. Cao, and D. N. Christodoulides, Unidirectional Invisibility Induced by P T -Symmetric Periodic Structures, *Phys. Rev. Lett.* 106, 213901 (2011).
- [7] H. Hodaei, A. U. Hassan, S. Wittek, H. Garcia-Gracia, R. El-Ganainy, D. N. Christodoulides, and M. Khajavikhan, Enhanced Sensitivity at Higher-Order Exceptional Points, *Nature* 548, 187 (2017).
- [8] W. Chen, Ş. Kaya Özdemir, G. Zhao, J. Wiersig, and L. Yang, Exceptional Points Enhance Sensing in an Optical Microcavity, *Nature* 548, 192 (2017).

- [9] M. P. Hokmabadi, A. Schumer, D. N. Christodoulides, and M. Khajavikhan, Non-Hermitian Ring Laser Gyroscopes with Enhanced Sagnac Sensitivity, *Nature* 576, 70 (2019).
- [10] J.-H. Park, A. Ndao, W. Cai, L. Hsu, A. Kodigala, T. Lepetit, Y.-H. Lo, and B. Kanté, Symmetry-Breaking-Induced Plasmonic Exceptional Points and Nanoscale Sensing, *Nat. Phys.* 16, 462 (2020).
- [11] R. Uzdin, A. Mailybaev, and N. Moiseyev, On the Observability and Asymmetry of Adiabatic State Flips Generated by Exceptional Points, *J. Phys. A: Math. Theor.* 44, 435302 (2011).
- [12] G. Nenciut and G. Rasche, On the Adiabatic Theorem for Non-Self-Adjoint Hamiltonians, 12 (n.d.).
- [13] J. W. Yoon et al., Time-Asymmetric Loop around an Exceptional Point over the Full Optical Communications Band, *Nature* 562, 86 (2018).
- [14] W. Liu, Y. Wu, C.-K. Duan, X. Rong, and J. Du, Dynamically Encircling an Exceptional Point in a Real Quantum System, *Phys. Rev. Lett.* 126, 170506 (2021).
- [15] Y. Choi, C. Hahn, J. W. Yoon, S. H. Song, and P. Berini, Extremely Broadband, on-Chip Optical Nonreciprocity Enabled by Mimicking Nonlinear Anti-Adiabatic Quantum Jumps near Exceptional Points, *Nat Commun* 8, 14154 (2017).
- [16] A. Li et al., Hamiltonian Hopping for Efficient Chiral Mode Switching in Encircling Exceptional Points, *Phys. Rev. Lett.* 125, 187403 (2020).
- [17] X. Shu, A. Li, G. Hu, J. Wang, A. Alù, and L. Chen, Fast Encirclement of an Exceptional Point for Highly Efficient and Compact Chiral Mode Converters, *Nat Commun* 13, 2123 (2022).

- [18] H. Nasari, G. Lopez-Galmiche, H. E. Lopez-Aviles, A. Schumer, A. U. Hassan, Q. Zhong, S. Rotter, P. LiKamWa, D. N. Christodoulides, and M. Khajavikhan, Observation of Chiral State Transfer without Encircling an Exceptional Point, *Nature* 605, 256 (2022).
- [19] T. Schmiedl and U. Seifert, Efficiency at Maximum Power: An Analytically Solvable Model for Stochastic Heat Engines, *Europhys. Lett.* 81, 20003 (2008).
- [20] S. Iram et al., Controlling the Speed and Trajectory of Evolution with Counterdiabatic Driving, *Nat. Phys.* 17, 135 (2021).
- [21] M. Mitchell, *An introduction to genetic algorithms* (MIT press, 1998).
- [22] P.T. Boggs and J.W. Tolle, Sequential Quadratic Programming, *Acta Numerica* 4, 1 (1995).

Acknowledgments

The work at Zhejiang University was sponsored by the Key Research and Development Program of the Ministry of Science and Technology under Grant 2022YFA1405200, the National Natural Science Foundation of China (NNSFC) under Grants No. 92163123, 61625502, and 61975176, the Key Research and Development Program of Zhejiang Province under Grant No.2022C01036, and the Fundamental Research Funds for the Central Universities.

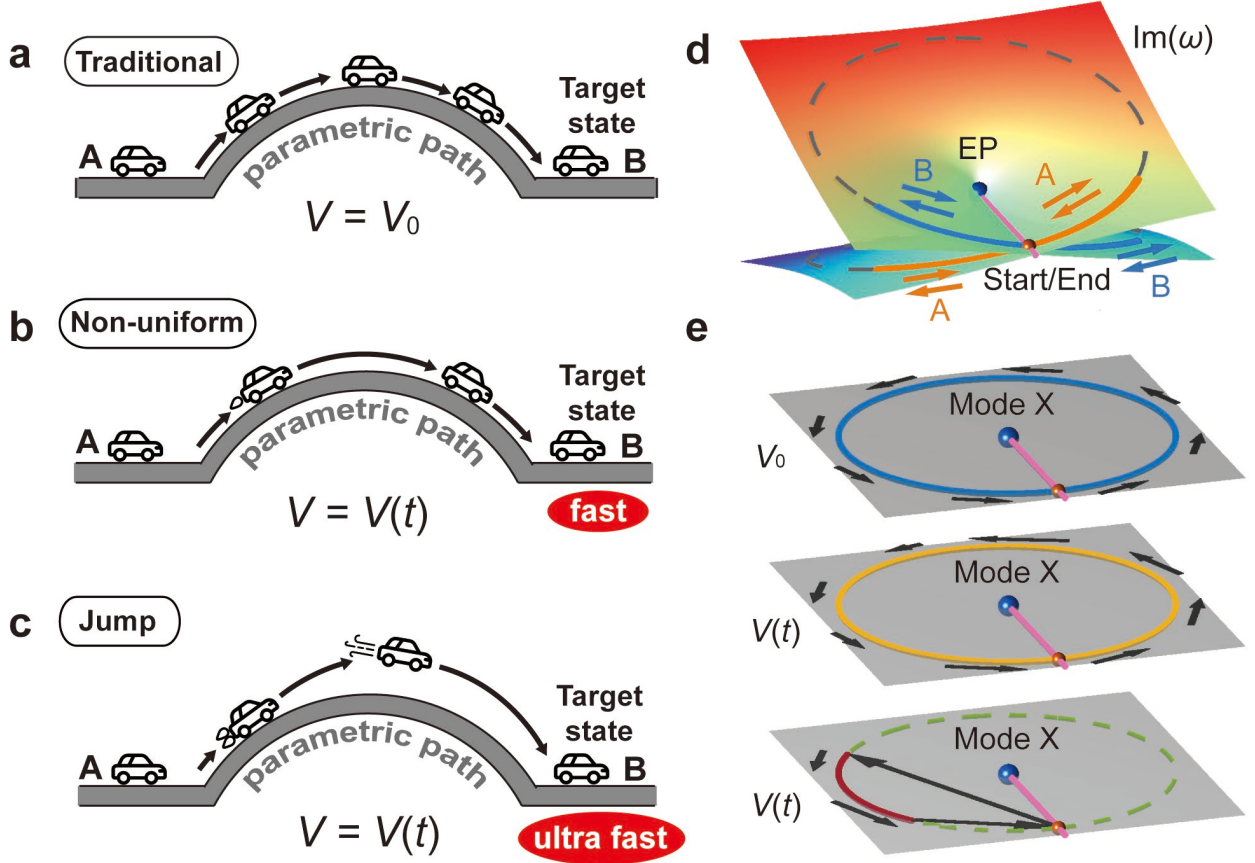


FIG. 1. The schematic diagram of fast mode conversion through adiabatic engineering on the parameter path. (a, b, c) show three different patterns for a car (system) to evolving from A to B. Adiabaticity indicates the car will not leave the surface of the arch bridge, which limits the car's velocity. Thus, the conventional dynamic evolution speed is slow and uniform (a). However, the maximum of velocity differs at different position, so we could design the nonuniform speed $v(t)$, which is the function of speed limitation along the path, to accelerate the evolution process (b). Moreover, if the end state is the chief objective, the adiabatic restriction can be loosened in some positions to obtain faster evolution speed (c). d is the imaginary Riemann surface of the non-Hermitian Hamiltonian in the main text. Orange (blue) arrows represent input or output mode A (B) in the parametric evolution. e shows uniform evolution (upper), nonuniform evolution (middle) and jump evolution (lower).

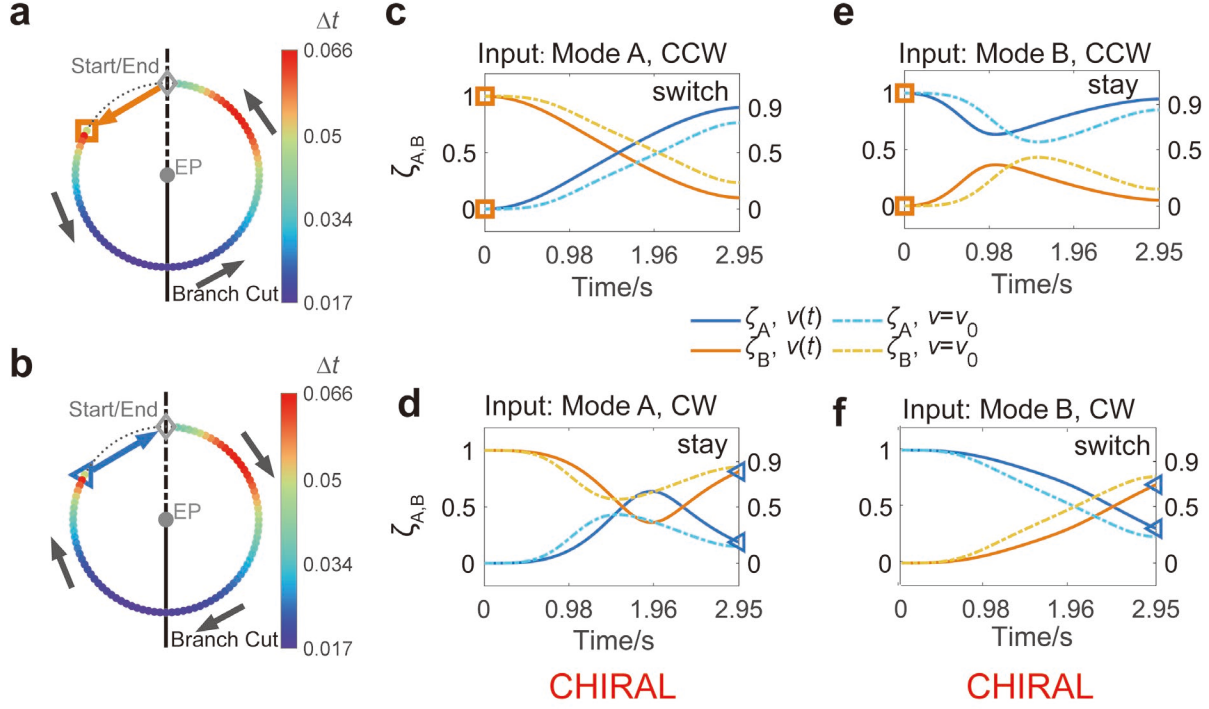


FIG. 2. **Bimodal chiral mode conversion in nonuniform evolution.** (a, b). The evolution time set $\{\Delta t_j\}$ of chiral cases and evolution patterns in parameter planes of CCW and CW directions. (c-f). Chiral mode conversion effect of the input mode A and mode B. For mode A, it will be switched to mode B in CCW evolution and maintained in CW evolution. While for mode B, it will be maintained in CCW evolution and switched to mode A in CW evolution.

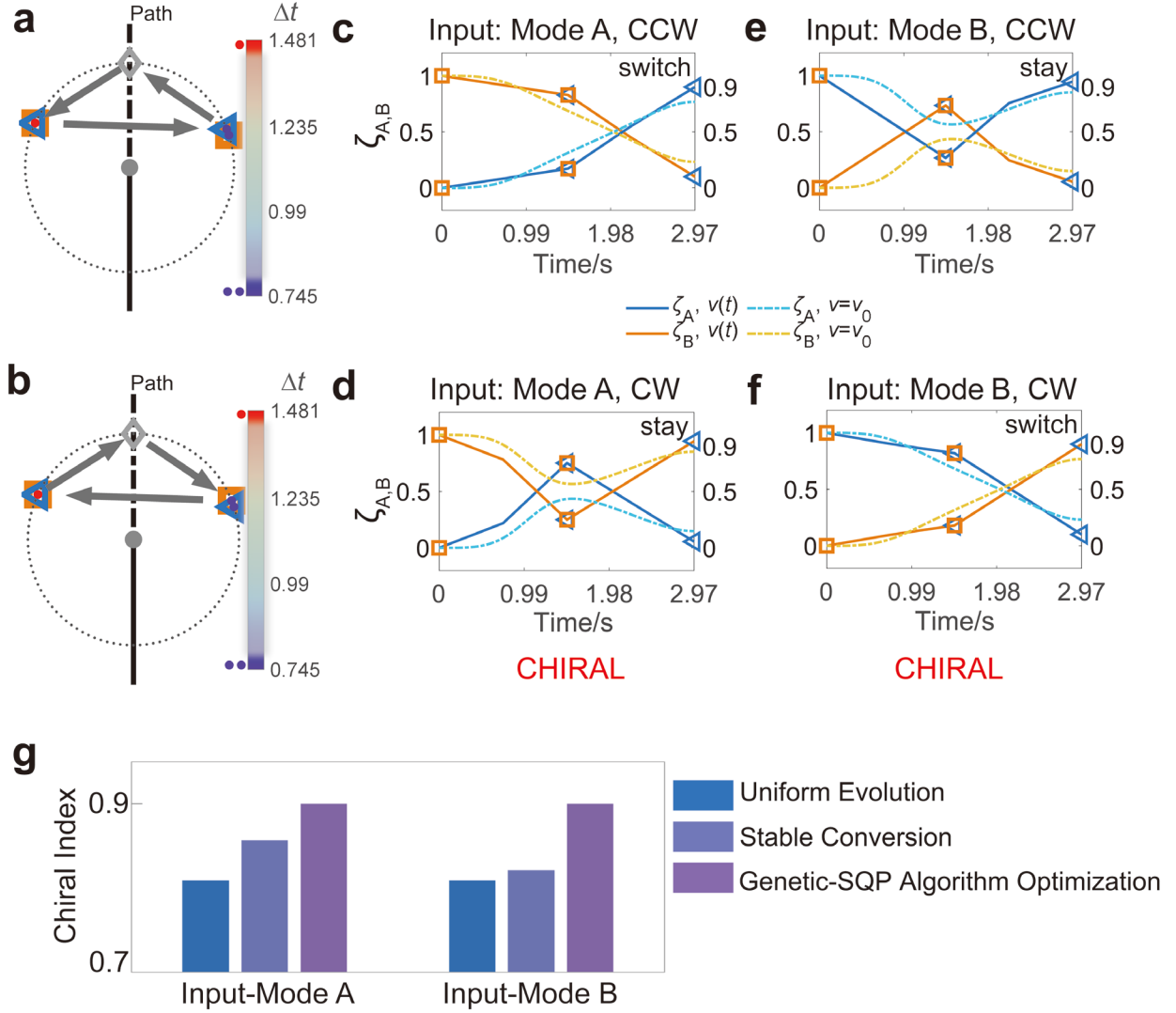


FIG. 3. **Bimodal chiral mode conversion under the optimization of genetic-SQP algorithm.**

(a, b). The evolution time set $\{\Delta t_j\}$ of chiral cases and evolution patterns in parameter planes of CCW and CW directions. Actually, the algorithm has skipped most of the path and just selects three parameter points to evolve (red and blue dots in a and b). (c-f). Chiral mode conversion effect of the input mode A and mode B. g shows the comparison of uniform evolution, stable conversion and genetic-SQP algorithm optimization methods in the chiral effect. Out optimized evolution shows great advantages in terms of evolution speed, end state purity, chiral effect and its robustness (chiral effect is independent of the input mode).

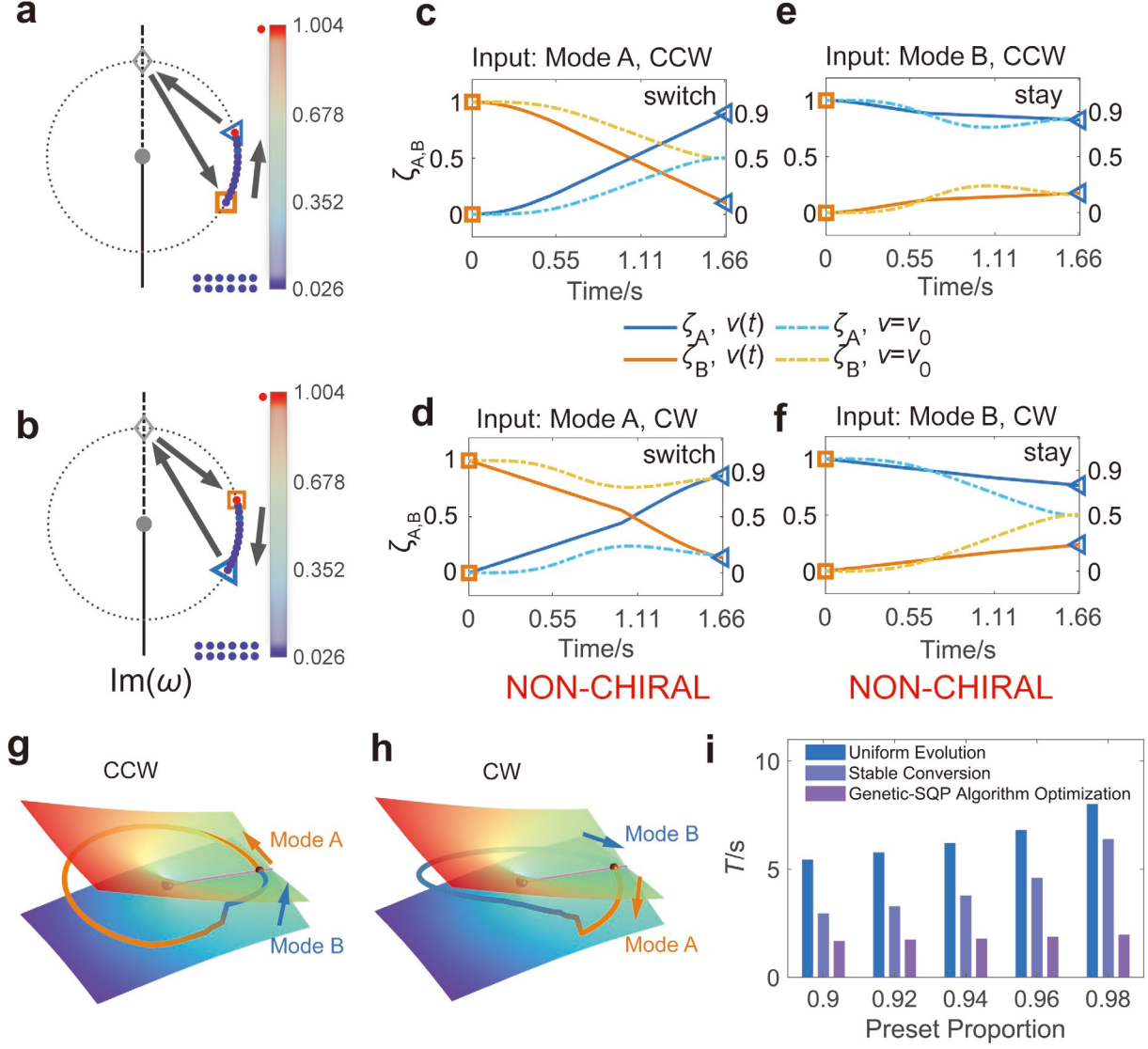


FIG. 4. **Bimodal non-chiral state evolution under the optimization of genetic-SQP algorithm.** (a, b). The evolution time set $\{\Delta t_j\}$ of non-chiral cases and evolution patterns in parameter planes of CCW and CW directions. The algorithm selects a length of path to evolve (red and blue dots in a and b) in this case. (c-f). Non-chiral state evolution effect of the input mode A and mode B. (g, h). The change of the weighted eigenvalue $\text{Im}(\bar{\omega})$ of system's state in Riemann surfaces of CCW and CW for the input mode A. The orange part means the mode A dominates

and the blue part means the mode B dominates. (i). Comparison of time consumption for three evolution method to realize mode conversion with different requirement of final state purity.